ELSEVIER

Biochimica et Biophysica Acta 1320 (1997) 34–44

BIOCHIMICA ET BIOPHYSICA ACTA
BBA

Evidence for multiple steps in the pre-steady-state electron transfer reaction of nitrogenase from *Azotobacter vinelandii*

Martina G. Duyvis, Richard E. Mensink, Hans Wassink, Huub Haaker *

Department of Biochemistry, Wageningen Agricultural University, Dreijenlaan 3, 6703 HA Wageningen, The Netherlands

Received 6 November 1996; revised 15 January 1997; accepted 16 January 1997

Abstract

The effect of the NaCl concentration and the reaction temperature on the MgATP-dependent pre-steady-state electron transfer reaction (from the Fe protein to the MoFe protein) of nitrogenase from *Azotobacter vinelandii* was studied by stopped-flow spectrophotometry and rapid-freeze EPR spectroscopy. Besides lowering the reaction temperature, also the addition of NaCl decreased the observed rate constant and the amplitude of the absorbance increase (at 430 nm) which accompanies pre-steady-state electron transfer. The diminished absorbance increase observed at 5°C (without NaCl) can be explained by assuming reversible electron transfer, which was revealed by rapid-freeze EPR experiments that indicated an incomplete reduction of the FeMo cofactor. This was not the case with the salt-induced decrease of the amplitude of the stopped-flow signal: the observed absorbance amplitude of the electron transfer reaction predicted only 35% reduction of the MoFe protein, whereas rapid-freeze EPR showed 80% reduction of the FeMo cofactor. In the presence of salt, the kinetics of the reduction of the FeMo cofactor showed a lag period which was not observed in the absorbance changes. It is proposed that the pre-steady-state electron transfer reaction is not a single reaction but consists of two steps: electron transfer from the Fe protein to a still unidentified site on the MoFe protein, followed by the reduction of the FeMo cofactor. The consequences of our finding that the pre-steady-state FeMo cofactor reduction does not correlate with the amplitude and kinetics of the pre-steady-state absorbance increase will be discussed with respect to the present model of the kinetic cycle of nitrogenase.

Keywords: Nitrogenase; Pre-steady-state electron transfer; Reversibility of ATPase reaction

1. Introduction

Nitrogenase is the enzyme complex which catalyses the reduction of dinitrogen to ammonia. The nitrogenase complex comprises two metalloproteins, the MoFe protein and the Fe protein, which are both necessary for catalysis, as well as MgATP and a strong reductant [1]. The crystal structures of both nitrogenase proteins have been solved [2–6]. The MoFe protein (Av1), is a tetramer ($\alpha_2\beta_2$) of 230 kDa. Each $\alpha\beta$-unit represents a catalytically independent moiety which contains one iron-molybdenum cofactor (FeMoco) and one P-cluster. FeMoco is thought to be the catalytic site for substrate reduction; the P-cluster is close to the putative Fe protein binding site and might be involved in intramolecular electron transfer to FeMoco [7]. There is some dis-

Abbreviations: Av1 and Av2, MoFe protein and Fe protein, respectively, of *Azotobacter vinelandii* nitrogenase; Kp1 and Kp2, MoFe protein and Fe protein, respectively, of *Klebsiella pneumoniae* nitrogenase.

* Corresponding author. Fax: +31 317 48 48 01; E-mail: huub.haaker@nitro@bc.wau.nl

PII S0005-2728(97)00006-6

cussion about the structure of the P-cluster [5,6]. The other nitrogenase protein, the Fe protein (Av2), is a homodimer of 63 kDa, which contains one [4Fe-4S] cluster and two binding sites for MgATP or MgADP [4].

A kinetic model for the reduction of dinitrogen to ammonia by nitrogenase was developed by Thorneley and Lowe [8,9]. The model consists of an Fe protein cycle and a MoFe protein cycle. The Fe protein cycle involves association of the Fe protein and the MoFe protein to form the nitrogenase complex, the subsequent transfer of a single electron from the Fe protein to the MoFe protein with concomitant hydrolysis of MgATP, followed by dissociation of the nitrogenase complex. The MoFe protein cycle describes the stepwise reduction of the MoFe protein by eight consecutive Fe protein cycles, required for the complete reduction of N_2 to 2 NH_3 and H_2.

Electron transfer from the Fe protein to the MoFe protein has been monitored by (rapid-freeze) EPR [10–13], following the decrease of the $S = 3/2$ EPR signal of FeMoco (*g*-values 4.3, 3.7 and 2.01), due to reduction of FeMoco and the decrease of the $S = 1/2$ EPR signal of the [4Fe-4S] cluster of the Fe protein (*g*-values 2.05, 1.94 and 1.89), due to oxidation of the Fe protein. Later, the electron transfer from the Fe protein to the MoFe protein was monitored also by stopped-flow spectrophotometry. The absorbance increase at 430 nm, observed after mixing of both nitrogenase proteins with MgATP, is mainly due to the oxidation of the Fe protein in the electron transfer reaction [14,15]. Lowering the reaction temperature (compared to room temperature) diminishes this absorbance increase at 430 nm [16,17]. Thorneley et al. [16] suggested that this effect can be explained by assuming that both electron transfer between the component proteins of nitrogenase and hydrolysis of MgATP are reversible processes; at a lower reaction temperature (6°C) the back reactions become more important, which causes the lower absorbance increase at 430 nm. Mensink and Haaker [17] have argued that the kinetic evidence indicates that only electron transfer might be regarded as a reversible reaction, but that the interaction of MgATP with nitrogenase is fast and irreversible.

Several studies have been conducted on the effects of salt on the properties and catalytic activity of the nitrogenase proteins and the complex. The $s_{20,w}$ value for the MoFe protein from *A. vinelandii* is increased by the presence of NaCl [18]. Binding of NaCl to the Fe protein from *A. vinelandii* is revealed by inhibition of the MgATP-dependent chelation of the iron-sulphur cluster by 2,2-bipyridyl [19]. Salts are also known to be inhibitory in steady-state substrate reduction assays for the nitrogenase complex [18,19]. A cross-linking study with the nitrogenase complex from *A. vinelandii* established that NaCl inhibits the association of the component proteins [20].

We report here that NaCl suppresses the absorbance increase at 430 nm associated with MgATP-dependent pre-steady-state electron transfer from the Fe protein to the MoFe protein. Rapid-freeze EPR data will be presented which show that the effect of NaCl cannot be attributed to incomplete reduction of FeMoco and that there is a lag in the reduction of FeMoco, which indicates that a reaction – made slower by the presence of NaCl – preceeds the reduction of FeMoco.

2. Materials and methods

2.1. Cell growth, isolation and preparation of nitrogenase

Azotobacter vinelandii ATCC strain 478 was grown and the nitrogenase component proteins were purified and assayed as described elsewhere [21]. Specific activities of Av1 and Av2 were at least 8 mol ethylene produced $\cdot s^{-1} \cdot$ mol protein^{-1} and 2 mol ethylene produced $\cdot s^{-1} \cdot$ mol protein^{-1}, respectively. Av1 contained 1.8 ± 0.2 Mo/mol Av1. The iron content of the Fe protein was 3.6 ± 0.3 mol Fe/mol Av2.

2.2. Stopped-flow and rapid-freeze methods

Stopped-flow spectrophotometry was performed with a HI-TECH SF-51 stopped-flow apparatus (Salisbury, Wilts, UK) equipped with an anaerobic kit, data acquisition and analysis system. The mixing ratio was 1:1. The absorbance changes were measured at 430 nm. In calculating the absorbance changes a dead reaction time of 1.5 ms was taken into account. Syringe one contained 20 μM Av1 and 120 μM Av2; the other syringe contained 10 mM

ATP. Both syringes contained 10 mM $MgCl_2$, 5 mM $Na_2S_2O_4$ and 50 mM Tes/NaOH, final pH 7.4. The concentration of NaCl, if present in the reaction mixture and the reaction temperature were as indicated in the figure legends.

Rapid-freeze experiments were performed with a home-built rapid-mixing apparatus, equipped with 2.5 ml Hamilton syringes (gastight), HPLC valves (Valco) and PEEK tubing (Upchurch Scientific) to connect the syringes with the mixing chamber and for the aging hose. The end of the aging hose was connected to a nozzle from which the reaction mixture sprayed into a funnel to which an EPR tube was connected with a rubber tubing. With the shortest delay line possible, the minimal reaction time was 17 ms. Both the funnel and EPR tube were immersed in a cold isopentane solution (≈ -140°C; the isopentane solution was cooled down with N_2(l) until the solution became viscous). The formed 'snow' was packed in the EPR tube and kept in liquid nitrogen for further analysis by EPR spectroscopy. EPR spectra were obtained with a Bruker EPR-200 D spectrometer, with periferal instrumentation and data acquisition as described elsewhere [22].

For the freeze experiments performed to study the effect of both a high salt concentration and a low reaction temperature, the reaction mixture was not sprayed in a cold isopentane solution, but, after a delay in the aging hose, pushed directly into an EPR tube. The argon flushed aging hose was just prior to the experiment inserted into the argon flushed and isopentane cooled EPR tube about three cm from the bottom of the tube. Inmediately after the experiment the tube was immersed into liquid N_2 cooled isopentane. No gas bubbles were present. The freezing time was determined from the reaction of oxidized myoglobin (Fe^{3+}) with sodium azide [23]: this was 500 ± 50 ms. The reproducibility of the different samples (± 5%, FeMoco signal) was better than with the spray method (± 15%, FeMoco signal).

In the (rapid-) freeze experiments one syringe of the rapid-mixing apparatus contained 40 μM Av1 and 240 μM Av2 and the other syringe contained 10 mM ATP. Both syringes contained 5 mM $Na_2S_2O_4$ and 10 mM $MgCl_2$ in 50 mM Tes/NaOH, final pH 7.4. The concentration of NaCl, if present in the reaction mixture and the reaction temperature were as indicated in the figure legends. Blanks were obtained by mixing a nitrogenase solution with buffer without MgATP.

The EPR conditions used for the measurements of the FeMoco $S = 3/2$ signal were: microwave frequency, 9.30 GHz; microwave power, 20 mW; modulation frequency, 100 kHz; modulation amplitude, 2.0 mT; temperature 6.3 K. The conditions used for the measurements of EPR signals of oxidized P-cluster were: microwave frequency, 9.18 GHz; microwave power, 200 mW; modulation frequency, 100 kHz; modulation amplitude, 2.0 mT; temperature 17 K. For the measurements of the Av2 $S = 1/2$ signal the EPR conditions were: microwave frequency, 9.18 GHz; microwave power, 31.7 mW; modulation frequency, 100 kHz; modulation amplitude, 1.25 mT; temperature 17 K.

The concentration of super-reduced FeMoco was calculated from the decrease (with respect to the amplitude at zero reaction time) in the amplitude of the $S = 3/2$ feature at $g = 3.64$ (since the experiments start with dithionite-reduced Av1, electron transfer from Av2 to Av1 causes 'super-reduction' of Av1). The decrease in the amplitude of the Av2 $S = 1/2$ signal at $g = 1.94$ was used to estimate the concentration of oxidized Av2. An accurate determination of the concentration of oxidized Av2 is hampered because binding of MgATP or MgADP to Av2 changes the shape of the $S = 1/2$ EPR signal and also causes a different distribution of the Av2 $S = 1/2$ and $S = 3/2$ spin-states [24]. The presence of Av1 also interferes with the Av2 $S = 1/2$ signal, because the FeMoco $S = 3/2$ signal has a g-value 2.0. Instead of double-integrating the whole Av2 $S = 1/2$ signal for quantification, we normalized the amplitude of the Av2 $g = 1.94$ feature of the obtained signals, to the amplitude at $g = 1.94$ of free Av2. The ratio between the amplitudes of the $g = 1.94$ feature of Av2 in the absence of a nucleotide, in the presence of MgATP and MgADP is 1: 0.995: 1.131, respectively (Hagen, W. F., personal communication). The error in the data points (see Table 1) was estimated from the difference in the EPR signals of three blanks.

The rate-limiting step(s) of nitrogenase catalysis was obtained from the specific acetylene reduction activity, determined with saturating Av2 ([Av2]/[Av1] = 20) and reductant (5 mM sodium dithionite plus 100 μM flavodoxin), at various salt

Table 1
The effect of the temperature and the salt concentration on the pre-steady-state electron transfer and on the redox state of FeMoco, as determined by stopped-flow spectrophotometry and EPR rapid-freeze spectroscopy

Condition and reaction time	Stopped-flow			EPR		
	k_{obs} rate-limiting step	k_{obs} electron transfer	ΔA_{430} (% of $\Delta A_{430(max)}$)	super-reduced FeMoco		oxidized Av2
				(%)	(μM)	(μM)
(A) 23°C, no NaCl (0.03 s)	4.6	159	98%	100%	36 ± 5	42 ± 25
(B) 23°C, 500 mM NaCl (0.5 s)	1.1	13.8	33%	83%	30 ± 5	51 ± 25
(C) 5°C, no NaCl (0.5 s)	0.08	7.1	35%	40%	14 ± 5	23 ± 25
(D) 5°C, 250 mM NaCl (8 s)	0.004	–	–	45%	16 ± 5	47 ± 25

In the stopped-flow experiments the concentrations after mixing were: Av1 = 10 μM (18 μM Mo) and Av2 = 60 μM (54 μM [4Fe-4S] cluster). In the rapid-freeze experiments the concentrations after mixing were: Av1 = 20 μM (36 μM Mo) and Av2 = 120 μM (108 μM [4Fe-4S] cluster). (A), (B), (C) and (D) correspond to traces A, B, C and D in Fig. 2. The k_{obs} of the rate-limiting step (calculated from the specific acetylene reduction activity) and the k_{obs} of electron transfer are expressed in s^{-1}. The calculated maximum absorbance increase $\Delta A_{430(max)} = 0.097$ [21]. At the reaction time (shown between brackets under 'condition') when the absorbance increase (ΔA_{430}) reached the observed maximum, the heights of the FeMoco $S = 3/2$ signal (at $g = 3.64$) and the Av2 $S = 1/2$ signal (at $g = 1.94$) were determined.

concentrations and reaction temperatures. It was checked that there was no significant H_2 evolution under all experimental conditions, thus the reported activities are a measure of the flux of electrons through nitrogenase. From the acetylene reduction activity a rate constant for the rate-limiting step(s) of nitrogenase catalysis was calculated.

All buffers used in the experiments were saturated with argon. ATP (special quality) was obtained from Boehringer.

3. Results

3.1. Effect of salt on the pre-steady-state absorbance changes

The electron transfer from the Fe protein to the MoFe protein can be monitored by stopped-flow spectrophotometry. Immediately after mixing of both nitrogenase proteins with MgATP (in the presence of a reductant) the absorbance at 430 nm increases due to the transfer of the first electron from the Fe protein to the MoFe protein. This absorbance increase is mainly caused by the absorbance change associated with the oxidation of the Fe protein in the electron transfer reaction [14,15]. The molecular absorbance coefficient for electron transfer from Av2 to Av1 is: $\epsilon_{430} = 5.4\ (\text{mM Mo})^{-1} \cdot \text{cm}^{-1}$ [17].

The effect of NaCl on the amplitude of the absorbance increase at 430 nm and the observed rate constant, associated with the electron transfer, is shown in Fig. 1A. NaCl decreased both the amplitude of the stopped-flow signal (ΔA_{430}) and the observed rate of electron transfer: a Hill plot for the effect of NaCl on the observed rate constant (k_{obs}) is given in Fig. 1B. The data fit to a Hill coefficient of 2.1, which suggests that the inhibition of NaCl on the observed rate of electron transfer occurs in a cooperative fashion. This is an indication that the electron transfer reaction should probably not be represented as a single electron transfer reaction.

No difference was observed between the stopped-flow traces obtained when the nitrogenase proteins were pre-equilibrated with NaCl before mixing with MgATP and the stopped-flow traces obtained when the nitrogenase proteins (without NaCl) were mixed MgATP and NaCl at once (data not shown). From these observations it must be inferred that the effect of NaCl is complete within the mixing time of the stopped-flow spectrophotometer. This implies that in the model of Deits and Howard [19] binding of NaCl to the nitrogenase complex and the subsequent dissociation of the component proteins must be fast.

The decrease of the observed rate constant and of the amplitude of the absorbance increase associated with the pre-steady-state electron transfer by NaCl, might be caused by inhibition of the association of the nitrogenase proteins in the presence of salt [20]. To verify this hypothesis, the effect of the ratio

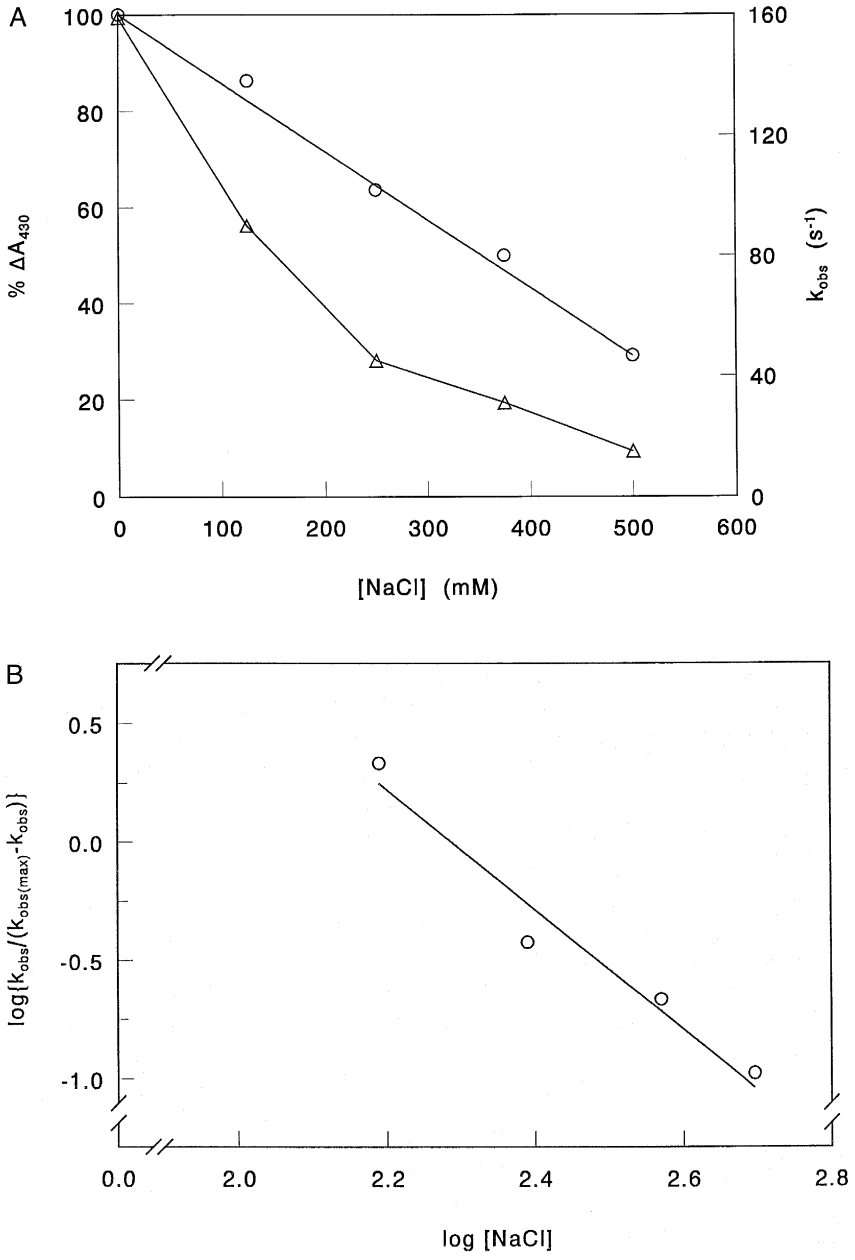

Fig. 1. Effect of the NaCl concentration on the absorbance change (430 nm) and the observed rate constant associated with electron transfer. The reaction temperature was 23.0 ± 0.1°C. A: the absorbance increase (ΔA_{430}) (○); and observed rate constant (k_{obs}) (△); caused by the MgATP-dependent electron transfer from Av2 to Av1. The maximum absorbance change, obtained in the absence of NaCl, is: $\Delta A_{430(max)} = 0.097$ ([Av1] = 10 μM). B: a Hill plot for the observed rate constant (k_{obs}) of the MgATP-dependent electron transfer. The rate constant observed in the absence of NaCl is: $k_{obs} = 159\ s^{-1}$.

[Av2]/[Av1] on k_{obs} and ΔA_{430} was studied in the absence and presence of NaCl. Av1 is an $\alpha_2\beta_2$-tetramer and each αβ-dimer contains one FeMoco and one binding site for Av2. In the absence of salt, the maximum pre-steady-state electron transfer (maximum ΔA_{430}) would be expected at a ratio [Av2]/[Av1] = 2. However, this is not the case: to obtain the maximum amplitude a higher ratio [Av2]/[Av1] is necessary. To explain their observation that the specific activity of the Fe protein from *Klebsiella pneumoniae* is only 45% of the calculated value, Thorneley and Lowe [25] assumed that only

45% of all Kp2 present is active. The remaining 55% is considered to be capable of binding to Kp1 (with lower rate constants for association and dissociation than active Kp2), but is inactive with respect to electron transfer. This assumption also explains the need for a ratio [Kp2]/[Kp1] ≥ 4.5 to obtain maximum electron transfer [26]. The nitrogenase proteins from *A. vinelandii* show the same phenomenon. The maximum value for ΔA_{430} was obtained at [Av2]/[Av1] = 6, both in the absence and presence of 250 mM NaCl, at 23°C (data not shown). Thus, it must be concluded that NaCl has no effect on the ratio [active Av2]/[inactive Av2]. However, the absorbance change in the presence of 250 mM NaCl with [Av2]/[Av1] ≥ 6 was only $\Delta A_{430} = 0.063$ (see Fig. 1A), which corresponds with $\epsilon_{430} = 3.5 \pm 0.3$ (mM Mo)$^{-1} \cdot$ cm^{-1} ([Av1] = 10 μM). This value differs significantly from the value of $\epsilon_{430} = 5.4 \pm 0.3$ (mM Mo)$^{-1} \cdot$ cm^{-1} which was obtained in the absence of NaCl [17]. In the presence of 250 mM NaCl, the observed rate constants increased from 23 s^{-1} at a ratio [Av2]/[Av1] = 1 to 34 s^{-1} at [Av2]/[Av1] = 12 (data not shown). In this experiment the protein concentration ([Av1] = 5 μM) was lower than in the experiment of Fig. 1A ([Av1] = 10 μM). In the experiment of Fig. 1A, at 250 mM NaCl, electron transfer occurred with $k_{obs} = 45$ s^{-1} ([Av2]/[Av1] = 6). If the concentrations of the nitrogenase proteins are low (< 0.5 μM), the so-called dilution effect occurs: the specific activity decreases as the total protein concentration decreases. This effect is due to the rate of association of the (reduced) Fe protein with the MoFe protein becoming rate-limiting at low protein concentrations [27]. Evidently, in the presence of 250 mM NaCl the dilution effect on nitrogenase activity is significant at [Av1] = 5 μM. NaCl affects nitrogenase activity by binding to the Fe protein and inhibition of the formation of the nitrogenase complex [19]. The lower observed rate constants of electron transfer at low protein concentrations and at low ratios [Av2]/[Av1] can therefore be explained by an initially smaller amount of binding sites on Av1 being occupied by Av2. During the electron transfer reaction the non-occupied Av2 binding sites on Av1 will eventually also bind Av2, which results in electron transfer. This lowers the observed rate constant of the electron transfer reaction. Without salts there is no additional complex formation at the time scale of the electron transfer reaction. The observed rate constant of electron transfer did not change with the ratio [Av2]/[Av1] if salt was absent from the reaction mixture (data not shown), which must probably be attributed to a larger fraction of Av1 which is complexed to Av2.

3.2. Relation between the absorbance changes and the redox state of the metal-sulphur clusters

A decrease of the reaction temperature (in the absence of NaCl) leads to a decrease of the absorbance amplitude and the observed rate constant of electron transfer. This effect on the stopped-flow signal was described earlier [16,17]. It was suggested that electron transfer from the Fe protein to the MoFe protein is reversible at lower temperatures (5°C) and mainly irreversible above 20°C. This would explain the diminished absorbance increase and observed rate constant at lower reaction temperatures.

Fig. 2 summarizes the influence of the NaCl concentration and the reaction temperature on the absorbance changes at 430 nm, observed after mixing of the nitrogenase proteins with MgATP. Note that the traces A, B, C and D in Fig. 2 have different time-axes.

The EPR rapid-freeze technique was used to check whether reversible electron transfer is manifested in the redox state of the nitrogenase proteins at a low reaction temperature or a high NaCl concentration. It must be realized that the protein concentrations used in the EPR rapid-freeze experiments are two times higher than in the stopped-flow experiments.

Table 1 combines the results of stopped-flow and rapid-freeze EPR experiments.

At 23°C, in the absence of NaCl, the absorbance increase (see Fig. 2, curve A) could be fitted to a single exponential: $\Delta A_{430} = 0.095$, with a rate constant $k_{obs} = 159$ s^{-1}. The absorbance increase was 98% of the calculated maximum value ($\Delta A_{430(max)} = 0.097$, [Av1] = 10 μM), see Table 1. The stopped-flow data predicted almost complete reduction of FeMoco. This was confirmed by the EPR rapid-freeze data: all FeMoco (36 μM) was super-reduced at the time when the absorbance maximum was reached (30 ms). The specific activity was 1200 nmol $C_2H_2 \cdot$ min$^{-1} \cdot$ mg^{-1} protein, from which the rate constant of the rate-limiting step of catalysis (at 23°C, in the

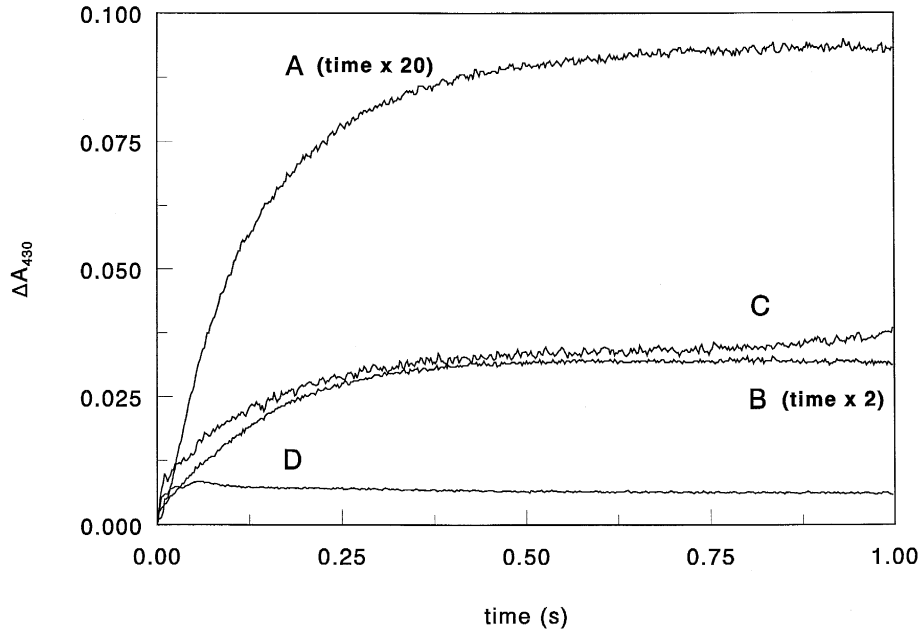

Fig. 2. The influence of the temperature and the salt concentration of the reaction mixture on the absorbance changes (ΔA_{430}). A and B were obtained at 23.0 ± 0.1°C; C and D at 5.0 ± 0.1°C. Reaction mixture (A) and (C) did not contain salt, (B) contained 500 mM NaCl and (D) contained 250 mM NaCl. The traces have different time-axes: the time-axis of trace (A) and trace (B) was multiplied by a factor 20 and 2, respectively (the actual time span of the traces was 50 ms and 0.5 s, respectively), whereas traces (C) and (D) are real 1 s traces.

absence of salt) was calculated: $k_{obs} = 4.6\ s^{-1}$, see Table 1.

At 23°C in the presence of 500 mM NaCl (Fig. 2, curve B), the absorbance increase was 33% of the calculated maximum absorbance increase ($\Delta A_{430} = 0.032$), with $k_{obs} = 13.8\ s^{-1}$. The specific activity was 25% of the specific activity in the absence of NaCl, at 23°C, resulting in $k_{obs} = 1.1\ s^{-1}$ for the rate-limiting step. The expected super-reduction of FeMoco was not confirmed by the rapid-freeze EPR measurements: at 0.5 s after mixing 83% of FeMoco was super-reduced, whereas, based on the observed absorbance increase, super-reduction of only 33% of FeMoco was expected.

At 5°C, in the absence of NaCl (Fig. 2, curve C), the absorbance increase was 35% of the calculated maximum value ($\Delta A_{430} = 0.034$) with $k_{obs} = 7.1\ s^{-1}$. At 0.5 s after mixing, the amount of super-reduced FeMoco, judged by the rapid-freeze EPR data, fairly corresponded with the prediction of the reduction of 35% of all FeMoco present: 40% of the FeMoco $S = 3/2$ signal had disappeared. The specific acetylene reduction activity was only 2% of the specific activity observed at 23°C, resulting in $k_{obs} = 0.08\ s^{-1}$ for the rate-limiting step.

When the reaction temperature was 5.0°C and 250 mM NaCl was present in the reaction mixture, hardly any activity was measured: $k_{obs} = 0.004\ s^{-1}$ for the rate-limiting step (see Table 1). Small absorbance changes could still be observed, see Fig. 2, curve D and Fig. 3. Immediately after mixing of the nitrogenase proteins with MgATP the absorbance increased with $\Delta A_{430} = 0.011$ and $k_{obs} = 199\ s^{-1}$ (see Fig. 2, curve D). The rate constant of this absorbance increase is too high to be related to electron transfer from the Fe protein to the MoFe protein at this low reaction temperature [17] and high salt concentration. This absorbance increase might be associated with the binding of MgATP to the nitrogenase complex. After 50 ms the absorbance increase was followed by a small decrease, with $\Delta A_{430} = 0.002$ and $k_{obs} = 1.1\ s^{-1}$. After the absorbance decrease some minor absorbance changes were observed. The rapid-freeze EPR measurements however indicated significant super-reduction of FeMoco, see Table 1.

In the absence of salt, the absorbance increase at

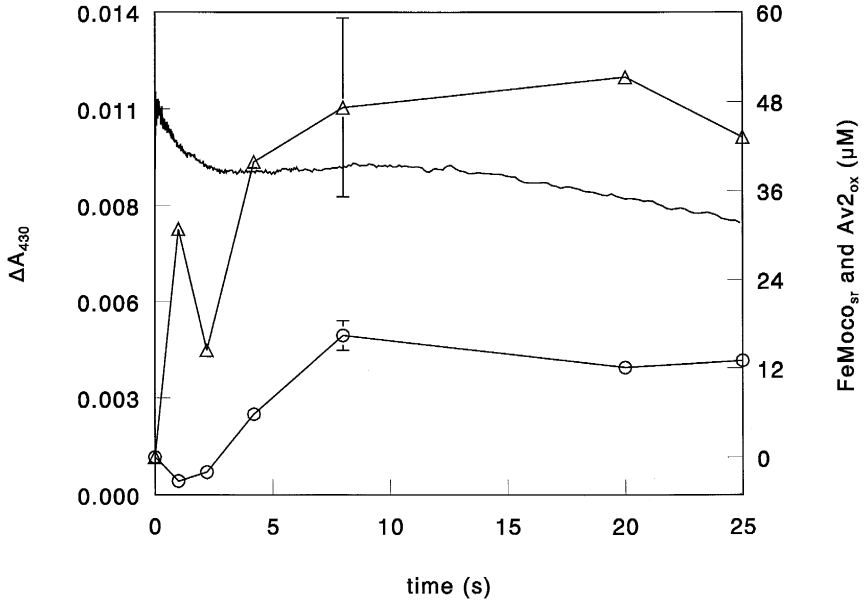

Fig. 3. The absorbance changes (ΔA_{430}) and the super-reduction of FeMoco at 5°C in the presence of 250 mM NaCl. The reaction mixtures in the stopped-flow and the rapid-freeze experiments contained 250 mM NaCl; the reaction temperature was 5.0 ± 0.2°C. From the rapid-freeze EPR data the amount of super-reduced FeMoco ($FeMoco_{sr}$) (○); and oxidized Av2 ($Av2_{ox}$) (△) were determined. The error bar given on one data point is representative of the error on each of the rapid-freeze EPR data points.

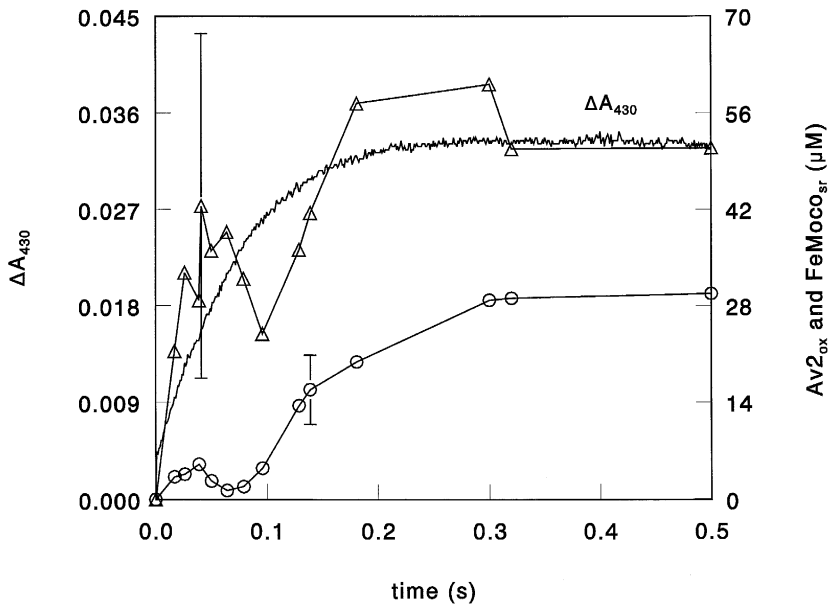

Fig. 4. The difference between the kinetics of the absorbance changes (ΔA_{430}) and the kinetics of the super-reduction of FeMoco, at 23°C in the presence of 500 mM NaCl. Both in the stopped-flow and the rapid-freeze EPR experiment the reaction mixture contained 500 mM NaCl; the reaction temperature was 23.0 ± 0.2°C. The calculated maximum absorbance change is $\Delta A_{430(max)} = 0.097$. From the rapid-freeze EPR data the amount of super-reduced FeMoco ($FeMoco_{sr}$) (○); and oxidized Av2 ($Av2_{ox}$) (△); were determined. The error bar given on one data point is representative of the error on each of the rapid-freeze EPR data points.

430 nm is a good measure of the electron transfer from the Fe protein to FeMoco at the MoFe protein. However, in the presence of NaCl, the absorbance increase does not give a good estimation of the amount of super-reduced FeMoco.

The kinetics of the super-reduction of FeMoco was studied in more detail by rapid-freeze EPR. Since the lowest reaction time in the rapid-freeze experiment was ≈ 17 ms (see Section 2) we did not attempt to determine the kinetics of the super-reduction of FeMoco at 23°C without NaCl. At 23°C in the presence of 500 mM NaCl, the kinetics of the decrease of the FeMoco $S = 3/2$ signal was different from the kinetics of the absorbance increase, see Fig. 4. The absorbance increase started immediately after mixing of the nitrogenase proteins with MgATP, whereas the FeMoco $S = 3/2$ signal started to decrease only after a delay of about 100 ms. The oxidation of Av2 went together with the absorbance increase, see Fig. 4. At 5°C without NaCl, the super-reduction of FeMoco went together with the increase of the stopped-flow signal (data not shown). At 5°C, in the presence of 250 mM NaCl, the FeMoco $S = 3/2$ signal started decreasing after a delay of 2 s (after mixing of the nitrogenase proteins with MgATP), indicating electron transfer to or from FeMoco, see Fig. 3. From 8 s after mixing the height of the FeMoco $S = 3/2$ signal remained more or less constant, at about 55% of its height at zero reaction time (see Table 1 and Fig. 4). The Av2 $S = 1/2$ signal started decreasing immediately after mixing of the nitrogenase proteins with MgATP. No indication of EPR signals of oxidized P-clusters as reported by Pierik et al. [28] and Tittsworth and Hales [29], or other signals (in perpendicular and parallel mode EPR) were found in the EPR samples during the reaction.

4. Discussion

The pre-steady-state absorbance increase (at 430 nm) has been used to monitor the electron transfer from the Fe protein to the MoFe protein of nitrogenase: the oxidation of the [4Fe-4S] cluster of the Fe protein and the super-reduction of FeMoco of the MoFe protein. The absorbance increases because the molecular absorbance coefficient of the redox change of the Fe protein is at least five times larger than the molecular absorbance coefficient of the MoFe protein upon reduction [26]. The lower absorbance increase as observed at a low reaction temperature (5°C) was explained by a reversible electron transfer between the Fe protein and the MoFe protein (as proposed by Thorneley et al. [16] and Mensink and Haaker [17]). Also in the presence of NaCl only a partial electron transfer reaction is predicted from stopped-flow spectrophotometry. The results of the rapid-freeze EPR experiments, however, indicated significantly more super-reduction of FeMoco under these circumstances and therefore reversible electron transfer between the nitrogenase proteins cannot account for the diminished absorbance change.

As explained in Materials and methods, the amount of oxidized Av2 cannot be determined accurately from the rapid-freeze EPR measurements. The shape of the Av2 $S = 1/2$ signal and the distribution of the Av2 $S = 1/2$ and $S = 3/2$ spin states change when MgATP or MgADP binds to Av2 [24]. The FeMoco $S = 3/2$ signal has a g-value 2.0, which interferes with the Av2 $S = 1/2$ signal. This makes quantification of the Av2 $S = 1/2$ signal (by double-integration) highly problematic. However, the amplitude of the $g = 1.94$ feature does not vary too much whether Av2 is free, MgATP- or MgADP-bound and was used (after normalizing for the amplitude of free Av2) for quantification. The next reason also makes the Av2 data points less accurate than the FeMoco data points. A ratio [Av]/[Av1] = 6 had to be used to saturate the electron transfer reaction; therefore Av2 is partially oxidized under standard conditions whereas almost all FeMoco can be super-reduced. The large scatter (Fig. 4, Table 1) in the Av2 data points might also be caused by a change of the distribution of the Av2 $S = 1/2$ and $S = 3/2$ spin states during freezing of the EPR samples. All this makes a calculation of oxidation of the Fe protein not accurate.

We would like to explain the data presented in this paper with our present scheme of the ATPase reaction of nitrogenase [30], see Scheme 1. After binding of MgATP to the nitrogenase proteins and subsequent change of the conformation of the nitrogenase complex to the MgATP-bound conformation, Av2 transfers one electron to Av1: $\epsilon_{430} = 5.4$ (mM Mo)$^{-1} \cdot$ cm^{-1} [17]. After electron transfer MgATP is hydrolyzed and the conformation of the nitrogenase com-

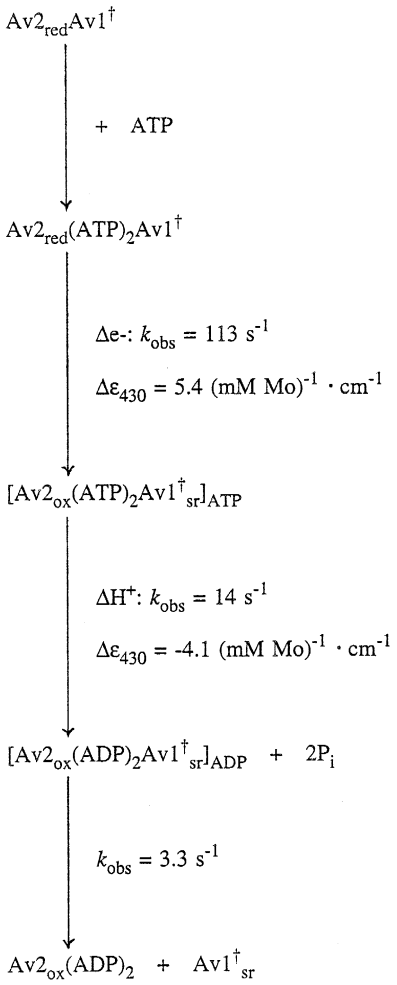

Scheme 1. Pre-steady-state reactions of nitrogenase with MgATP. All rate constants were measured for *A. vinelandii* nitrogenase. $Av1^{\dagger}$: one of two independently functioning halves of the MoFe protein; $Av1^{\dagger}_{sr}$: MoFe protein with super-reduced FeMoco, $Av2_{red}$ and $Av2_{ox}$: reduced and oxidized Fe protein, respectively; $[Av2(ATP)_2Av1^{\dagger}]_{ATP}$ or $[Av2(ADP)_2Av1^{\dagger}]_{ADP}$: the nitrogenase complex is in the MgATP-bound or MgADP-bound conformation, respectively; $\Delta e-$: electron transfer from the Fe protein to the MoFe protein is observed; ΔH^{+}: proton production is observed; $\Delta\epsilon_{430}$: an absorbance change at 430 nm is observed. The observed rate constants apply for the reactions at 20°C.

plex changes to the MgADP-bound conformation, which causes a decrease of the absorbance at 430 nm: $\epsilon_{430} = -4.1\ (\text{mM Mo})^{-1} \cdot \text{cm}^{-1}$. This reaction is followed by dissociation of the nitrogenase complex.

The effect of salt on the kinetics of the electron transfer from Av2 to Av1 can be explained by assuming that the change of the nitrogenase complex to the MgATP-bound conformation and the consequent electron transfer reaction are inhibited by the presence of salt; the hydrolysis of MgATP and subsequent change of the nitrogenase complex to the MgADP-bound conformation are less inhibited. The absorbance increase associated with electron transfer from Av2 to Av1 does not reach the calculated maximum value, because it is overtaken by the subsequent absorbance decrease, associated with the change to the MgADP-bound conformation of the nitrogenase complex.

The difference in the kinetics of the absorbance increase and of the super-reduction of FeMoco when 500 mM NaCl is present at 23°C (Fig. 4), as well as the delay of the super-reduction of FeMoco at 5°C with 250 mM NaCl present (Fig. 3), both indicate that the electron transfer reaction is not a single one-electron transfer from the [4Fe-4S] cluster of Av2 directly to FeMoco. It is possible that another redox site is involved in the electron transfer reaction. This primary electron acceptor of Av2 might be the P-cluster, as proposed by Peters et al. [7], but we did not observe any EPR signals confirming this proposal. It has been suggested in the literature that, as all iron atoms of the P-cluster are in the ferrous state [31], the disulfide bridge of the P-cluster might be reduced during catalysis [1,5].

At 5°C both the electron transfer from Av2 to Av1 and the conformational change of the nitrogenase complex after MgATP hydrolysis (to the MgADP-bound conformation) become slower. Reversibility of the electron transfer reaction might well be the cause of the diminished absorbance increase and the partial super-reduction of FeMoco.

At 5°C in the presence of 250 mM NaCl (Fig. 3), electron transfer to or from FeMoco occurred although no increase of the absorbance was observed. Both the temperature effect and the salt effect contribute to the lowering of the amplitude of the stopped-flow signal.

Acknowledgements

We thank Prof. W.R. Hagen for performing the EPR spectroscopy and Prof. C. Veeger and Prof. C. Laane for critically reading this manuscript. This investigation was supported by the Netherlands Foundation for Chemical Research (SON) with financial

aid from the Netherlands Organization for Scientific Research (NWO).

References

[1] Howard, J.B. and Rees, D.C. (1994) Annu. Rev. Biochem. 63, 235–264.
[2] Kim, J. and Rees, D.C. (1992) Science 257, 1677–1682.
[3] Kim, J. and Rees, D.C. (1992) Nature 360, 553–560.
[4] Georgiadis, M.M., Komiya, H., Chakrabarti, P., Woo, D., Kornuc, J.J. and Rees, D.C. (1992) Science 257, 1653–1659.
[5] Chan, M.K., Kim, J. and Rees, D.C. (1993) Science 260, 792–794.
[6] Bolin, J.T., Campobasso, N., Muchmore, S.W., Morgan, T.V. and Mortenson, L.E. (1993) In: Molybdenum Enzymes, Cofactors and Model Systems (Stiefel, E.I., Coucouvanis, D. and Newton, W.E., eds.) pp. 186–195, American Chemical Society, Washington.
[7] Peters, J.W., Fisher, K. Newton, W.E. and Dean, D.R. (1995) J. Biol. Chem. 270, 27007–27013.
[8] Thorneley, R.N.F. and Lowe, D.J. (1983) Biochem. J. 215, 393–403.
[9] Lowe, D.J. and Thorneley, R.N.F. (1984) Biochem. J. 224, 877–886.
[10] Orme-Johnson, W.H., Hamilton, W.D., Jones, T.L. Tso, M.-Y.W., Burris, R.H., Shah, V.K. and Brill, W.J. (1972) Proc. Natl. Acad. Sci. USA 69, 3142–3145.
[11] Smith, B.E., Lowe, D.J. and Bray, R.C. (1972) Biochem. J. 130, 641–643.
[12] Smith, B.E., Lowe, D.J. and Bray, R.C. (1973) Biochem. J. 135, 331–341.
[13] Zumft, W.G., Mortenson, L.E. and Palmer, G. (1974) Eur. J. Biochem. 46, 525–535.
[14] Thorneley, R.N.F. (1975) Biochem. J. 145, 391–396.
[15] Thorneley, R.N.F. and Cornish-Bowden, A. (1977) Biochem. J. 165, 255–262.
[16] Thorneley, R.N.F., Ashby, G., Howarth, J.V., Millar, N.C. and Gutfreund, H. (1989) Biochem. J. 264, 657–661.
[17] Mensink, R.E. and Haaker, H. (1992) Eur. J. Biochem. 208, 295–299.
[18] Burns, A., Watt, G.D. and Wang, Z.C. (1985) Biochemistry 24, 3932–3936.
[19] Deits, T.L. and Howard, J.B. (1990) J. Biol. Chem. 265, 3859–3867.
[20] Willing, A.H., Georgiadis, M.M., Rees, D.C. and Howard, J.B. (1989) J. Biol. Chem. 264, 8499–8503.
[21] Mensink, R.E., Wassink, H. and Haaker, H. (1992) Eur. J. Biochem. 208, 289–294.
[22] Pierik, A.J. and Hagen, W.R. (1991) Eur. J. Biochem. 195, 505–516.
[23] Ballou, D.P. and Palmer, G.A. (1974) Anal. Chem. 46, 1248–1253.
[24] Hagen, W.R., Eady, R.R., Dunham, W.R. and Haaker, H. (1985) FEBS Lett. 189, 250–254.
[25] Thorneley, R.N.F. and Lowe, D.J. (1984) Biochem. J. 224, 903–909.
[26] Ashby, G.A. and Thorneley, R.N.F. (1987) Biochem. J. 246, 455–465.
[27] Thorneley, R.N.F. and Lowe, D.J. (1984) Biochem. J. 224, 903–909.
[28] Pierik, A.J., Wassink, H., Haaker, H. and Hagen, W.R. (1993) Eur. J. Biochem. 212, 51–61.
[29] Tittsworth, R.C. and Hales, B.J. (1993) J. Am. Chem. Soc. 115, 9763–9767.
[30] Duyvis, M.G., Wassink, H. and Haaker, H. (1996) J. Biol. Chem., in press.
[31] Surerus, K.K., Hendrich, M.P., Christie, P.D., Rottgardt, D., Orme-Johnson, W.H. and Münck, E. (1992) J. Am. Chem. Soc. 114, 8579–8590.